Mon. Not. R. Astron. Soc. **368,** 741–750 (2006) doi:10.1111/j.1365-2966.2006.10161.x

The importance of interactions for mass loss from satellite galaxies in cold dark matter haloes

Alexander Knebe,[1⋆] Chris Power,[2] Stuart P. D. Gill[2,3] and Brad K. Gibson[4,5]

[1]*Astrophysikalisches Institut Potsdam, An der Sternwarte 16, 14482 Potsdam, Germany*
[2]*Centre for Astrophysics & Supercomputing, Swinburne University, Mail #39, PO Box 218, Hawthorn, Victoria 3122, Australia*
[3]*Department of Astronomy, Columbia University, 550 West 120th Street, New York, NY 10027, USA*
[4]*Laboratoire d'Astrophysique, Ecole Polytechnique Federale de Lausanne (EPFL), CH-1290 Sauverny, Switzerland*
[5]*Centre for Astrophysics, University of Central Lancashire, Preston PR1 2HE*

Accepted 2006 February 1. Received 2006 January 30; in original form 2005 July 15

ABSTRACT

We investigate the importance of interactions between dark matter substructures for the mass loss they suffer whilst orbiting within a sample of high-resolution galaxy cluster mass cold dark matter (CDM) haloes formed in cosmological N-body simulations. We have defined a quantitative measure that gauges the degree to which interactions are responsible for mass loss from substructures. This measure indicates that interactions are more prominent in younger systems when compared to older more relaxed systems. We show that this is due to the increased number of encounters a satellite experiences and a higher mass fraction in satellites. This is in spite of the uniformity in the distributions of relative distances and velocities of encounters between substructures within the different host systems in our sample.

Using a simple model to relate the net force felt by a single satellite to the mass loss it suffers, we show that interactions with other satellites account for ∼30 per cent of the total mass loss experienced over its lifetime. The relation between the age of the host and the importance of interactions increases the scatter about this mean value from ∼25 per cent for the oldest to ∼45 per cent for the youngest system we have studied. We conclude that satellite interactions play a vital role in the evolution of substructure in dark matter haloes and that a significant fraction of the tidally stripped material can be attributed to these interactions.

Key words: methods: N-body simulations – galaxies: clusters: general – galaxies: evolution – galaxies: formation.

1 INTRODUCTION

It has been understood for some time that the structure of a galaxy can be affected by tidal interactions with its close neighbour(s) (e.g. Toomre & Toomre 1972); telltale signs such as tidal tails and disturbed morphologies provide a visible record of these encounters. Around our own Galaxy, there is substantial evidence for its tidal interaction with the Small and Large Magellanic Clouds (SMC and LMC), the consequences of which have been studied in detail (e.g. Lin, Jones & Klemola 1995; Oh, Lin & Aarseth 1995; Gardiner & Noguchi 1996; Yoshizawa & Noguchi 2003; Bekki & Chiba 2005; Connors, Kawata & Gibson 2005; Mastropietro et al. 2005). Furthermore, an increasing number of studies have uncovered evidence for tidal stripping – in the form of stellar streams – in the Galactic halo (e.g. Ibata et al. 2003; Helmi 2004); these streams represent material that has been stripped from infalling satellites as they are disrupted by our Galaxy. The detection of such streams will become more commonplace in the coming years as the sensitivity of surveys improve (e.g. Odenkirchen et al. 2003; Navarro, Helmi & Freeman 2004), but there are already examples of stellar streams further afield, such as around M31 (Ibata et al. 2004). Moreover, Mihos et al. (2005) recently reported the discovery of intracluster light in the Virgo cluster, revealing several long (>100 kpc) tidal streamers.

These results represent compelling evidence that satellite galaxies tidally interact with their more massive hosts, and consequently lose some fraction of their mass. The effect of a satellite's interaction with its host and the mass loss it suffers has been studied in some detail (e.g. Hayashi et al. 2003), and it can be argued that it is relatively well understood. In comparison, the importance of a satellite galaxy's interactions with other satellite galaxies, the nature of these interactions and the contribution they make to its mass loss is less well understood. There is evidence to suggest that tidal interactions *between* satellite galaxies occur; Zhao (1998) and Ibata & Lewis (1998) investigated whether the Sagittarius Dwarf galaxy

⋆E-mail: aknebe@aip.de

could have experienced an encounter with the SMC and LMC some 2–3 Gyr ago, while the disturbed H I distribution noted by Yun, Ho & Lo (1994) in the M81 group is highly suggestive of tidal interactions between the group galaxies. Goto (2005) argues that tidal interaction between galaxies is the dominant mechanism driving cluster galaxy evolution and underpins the Butcher–Oemler effect and the morphology–density relation.

It has been understood for some time that dark matter haloes must play an important dynamical role in encounters between galaxies because they significantly reduce the merging time-scale (Barnes 1988). Examples of tidal interaction and merging are observed in relatively low-density environments (i.e. the field), but how reasonable is it to expect that interactions should be more common in higher density environments such as galaxy groups and clusters? Tidal interactions have been proposed as a mechanism for galaxy transformation in galaxy clusters, such as the 'harassment' scenario envisaged by Moore, Lake & Katz (1998), but what does the favoured paradigm for cosmological structure formation, the cold dark matter (CDM) model, predict?

The aim of this paper is to quantify the importance of satellite–satellite encounters and to assess their impact upon the transformation and mass loss of the substructure population within the context of the CDM model. We have drawn on a sample of high-resolution cosmological N-body simulations of cluster mass dark matter haloes and analysed the interactions of the substructure haloes (hereafter subhaloes) both with the host halo and with other subhaloes. We associate these subhaloes with the hosts of satellite galaxies (but see Gao et al. 2004) and in what follows, we use the terms subhalo and satellite (galaxy) interchangeably. The fine time sampling of our simulations allow us to follow the time evolution of subhalo properties in detail, and so we can determine the relative contributions of the host and the other subhaloes to changes in a subhalo's structure.

In a previous study (Knebe, Gill & Gibson 2004), we quantified the frequency of encounters between subhaloes orbiting within a common CDM cluster mass halo, considering the period between the halo's formation redshift[1] and the present day. We found that, on average, 30 per cent of the 'satellite galaxy' population experienced at least one encounter per orbit with another satellite galaxy. This result was sensitive to the age of the host halo, with a clear trend for more encounters in younger systems. We also reported a correlation between the number of encounters and halocentric radius – satellite galaxies closer to the centre of the host were measured to experience more interactions, although we note that this simply reflects the increasing spatial density of satellites with decreasing radius within a host halo.

The principal shortcoming of the approach adopted in Knebe et al. (2004) is that we neglected the relative velocities of the satellite galaxies; our satellites may have experienced encounters, but we had no information about their specific nature, i.e. were they fast or slow? Such information is important when considering the impact on the satellite's structure. In the present study, we elaborate on that work by including information about the relative velocities of the satellites. In other words, we can now estimate the *importance* of encounters in addition to the frequency with which they occur, allowing us to differentiate between *slow* encounters, which we expect to be extremely disruptive to the satellite structure, and *fast* encounters, whose impact are likely to be minimal. We define a quantitative measure for interactions, which we call the *integral interaction measure* (IIM), based upon the force acting on a satellite over a given period of time, i.e. the (induced) momentum change. Whereas before we could examine the number of encounters a satellite galaxy experienced per orbit, we may now study how the instantaneous force due to encounters acting on a satellite galaxy varies along its orbit and how this correlates with mass loss, thus providing a natural measure of the importance of mutual interactions between satellite galaxies.

In what follows, we motivate our choice of the IIM as a gauge for the importance of interactions between satellite galaxies, and present the results of our analysis of a suite of high-resolution cluster mass haloes that formed assuming the ΛCDM cosmology. We demonstrate the suitability of the IIM for our purposes by performing a series of experiments with 'cleaned' simulations, in which we track the detailed mass loss history of a single satellite galaxy in a host halo in which the substructure has been removed. Finally, we compare and contrast our results with those of previous studies, and comment on their observable consequences.

2 THE SIMULATIONS

Our analysis is based on a suite of eight high-resolution N-body simulations (Gill, Knebe & Gibson 2004a; Gill et al. 2004b) carried out using the publicly available adaptive mesh refinement code MLAPM (Knebe, Green & Binney 2001) in a standard ΛCDM cosmology ($\Omega_0 = 0.3$, $\Omega_\lambda = 0.7$, $\Omega_b h^2 = 0.04$, $h = 0.7$, $\sigma_8 = 0.9$). Each run focuses on the formation and evolution of a dark matter galaxy cluster containing of order one million particles, with mass resolution $1.6 \times 10^8\, h^{-1}\, M_\odot$ and force resolution $\sim 2\, h^{-1}$ kpc which is of the order 0.5 per cent of the host's virial radius. These simulations have the required resolution to follow the satellites within the very central regions of the host potential ($\geqslant$5–10 per cent of the virial radius) and the time resolution to resolve the satellite dynamics with good accuracy ($\Delta t \approx 170$ Myr). Such temporal resolution provides of order 10–20 time-steps per orbit per satellite galaxy, thus allowing these simulations to be used in a previous paper (Gill et al. 2004b) to accurately measure the orbital parameters of each individual satellite galaxy.

Substructure within these haloes is identified using the halo finder MHF (MLAPM's-halo-finder). MHF is based upon the N-body code MLAPM and acts with exactly the same accuracy as the N-body code itself; it is therefore free of any bias and spurious mismatch between simulation data and halo finding precision arising from numerical effects. We applied MHF to each of our eight host haloes at their formation time which is the redshift $z_{\rm form}$ where the halo contains half of its present day mass. We track the orbits of each of the satellites identified within and around the host halo from $z_{\rm form}$ until $z = 0$ and follow the evolution of their properties in great detail. For further details relating to the properties of the satellite galaxies, we refer the reader to the Gill et al. (2004a,b) and Gill, Knebe & Gibson (2005) series of papers.

3 THE ANALYSIS

In what follows, we have considered only those satellites that have completed at least one full orbit within their host halo, corresponding to more than 70 per cent of the subhaloes. The number distribution of orbits peaks at about one–two orbits with the tail extending to as many as four orbits for the older host haloes. A detailed discussion of the orbital properties (amongst others) of the substructure population can be found in Gill et al. (2004a).

[1] We defined this to be the redshift at which the mass of the most massive progenitor was half the system's present day mass; this was typically $z \sim 0.5$ for the haloes we examined.

We restricted our sample of satellites to those that contain at least 100 particles, which translates to a minimum mass of $M_{\rm sat} \geqslant 2 \times 10^{10}\, h^{-1}\, {\rm M}_{\odot}$. To ensure that our results are not affected by resolution effects, we checked that all results presented below are recovered when the lower mass limit is gradually increased; that is, we considered additional lower mass cuts corresponding to 200 and 400 particles and we can confirm that our results are unaffected.

3.1 Integral interaction measure

We begin by calculating the forces acting on each satellite galaxy i for each available snapshot of the simulation, treating it as a point particle with mass m. The force $F^i_{\rm host}$ exerted by the host halo and the force $F^i_{\rm sat}$ exerted by all other satellites are given as follow:

$$F^i_{\rm sat} = Gm_i \sum_{i \neq j} \frac{m_j}{|r_i - r_j|^2},$$

$$F^i_{\rm host} = Gm_i \frac{M_{\rm host}(< r_i)}{r_i^2}, \tag{1}$$

where m_i is the mass of satellite i and $M_{\rm host}(<r_i)$ the mass of the host interior to the satellite distance r_i. We need to stress that both these formulae assume spherical symmetry and hence are only approximations to the 'true' forces.

We define a so-called (dimensionless) 'integral interaction measure' – IIM – for each individual satellite galaxy as follows:

$${\rm IIM}^i = \frac{1}{T} \int_0^T \frac{F^i_{\rm sat}(t)}{F^i_{\rm host}(t)} {\rm d}t, \tag{2}$$

where we integrate over a time interval $[0, T]$, which is the time satellite i has spent within its host's virial radius. Here we also note that due to our definition the IIM values scale linearly with the 'average satellite mass'. The discrete nature of the time sampling of our data requires that the integral should be expressed as the following summation:

$${\rm IIM}^i = \frac{1}{t_{\rm now} - t_i} \sum_{t=t_i}^{t_{\rm now}} \frac{F^i_{\rm sat}(t_m)}{F^i_{\rm host}(t_m)} \Delta t, \tag{3}$$

where $t_{\rm now}$ is the age of the Universe at redshift $z = 0$, t_i the age of the Universe when the satellite enters the host halo and Δt the time difference between two consecutive outputs. We average the forces exerted by both the other satellites and the host halo over the consecutive outputs, i.e. $[t - \Delta t/2, t + \Delta t/2]$, or 'mid-point integration' of equation (2):

$$F^i_{\rm sat}(t_m) = \frac{1}{2}\left(F^i_{\rm sat}\left(t - \frac{\Delta t}{2}\right) + F^i_{\rm sat}\left(t + \frac{\Delta t}{2}\right)\right),$$

$$F^i_{\rm host}(t_m) = \frac{1}{2}\left(F^i_{\rm host}\left(t - \frac{\Delta t}{2}\right) + F^i_{\rm host}\left(t + \frac{\Delta t}{2}\right)\right). \tag{4}$$

The IIM, equation (3), can now be used as a quantitative measure for the relative strength of satellite–satellite encounters.

3.1.1 Application of the integral interaction measure

In Fig. 1, we present the IIM as defined by equation (3), for each satellite in our suite of eight host haloes plotted as a function of satellite mass. This figure suggests that there is no clear trend for interactions to correlate with mass, as we might have expected; it would be rather surprising to find that, for instance, high-mass satellites tend to interact more prominently than low-mass ones (or vice versa).

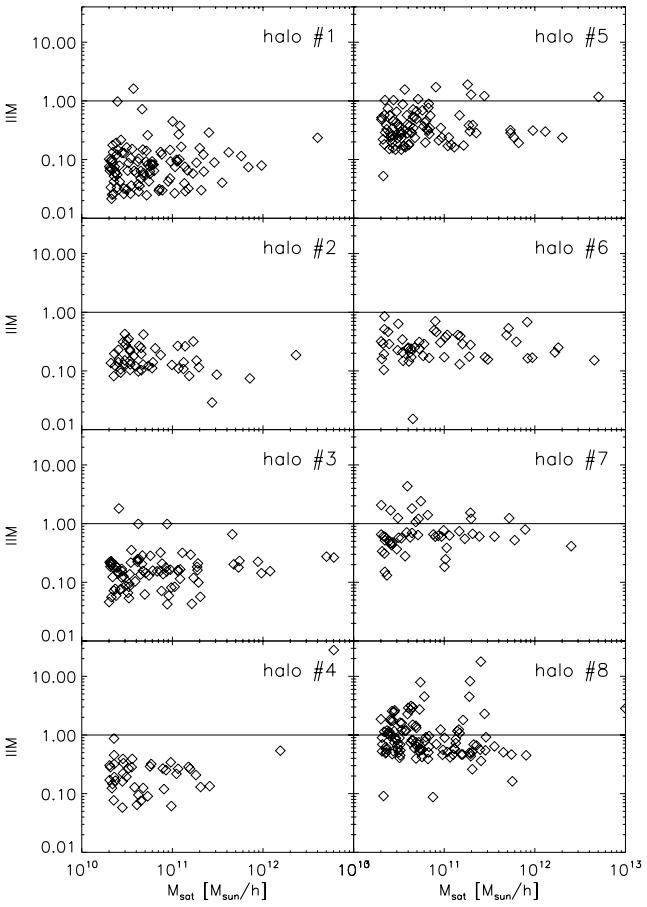

Figure 1. The IIM as a function of satellite mass.

The most striking feature of Fig. 1 is the apparent rise of the IIM values as a function of decreasing age for the host haloes: the haloes are ordered in age with halo # 1 being 8.3 Gyr old and halo # 8 a mere 3.4 Gyr.

This can be better viewed in Fig. 2 where we plot the distributions of the IIM. For all our eight host haloes these distributions have been fitted with a lognormal function

$$n({\rm IIM}) = \frac{1}{({\rm IIM}/{\rm IIM}_0)\sqrt{2\pi\sigma_0^2}} \exp\left(-\frac{\ln^2({\rm IIM}/{\rm IIM}_0)}{2\sigma_0^2}\right); \tag{5}$$

corresponding best-fitting parameters along with the halo age are listed in Table 1 where ${\rm IIM}_{\rm peak} = {\rm IIM}_0 \exp(-\sigma^2)$ for a lognormal distribution.

The increase of the IIM with decreasing age of the host is consistent with the behaviour observed in Knebe et al. (2004), in which it was noted that the tail of the distribution of the number of encounters per orbit extended to larger values for younger host systems. However, the result implied by the IIM is distinct from that presented in Knebe et al. (2004) in the sense that we are considering the net force acting on a subhalo over some time interval, whereas we previously considered encounters as events in which a pair of subhaloes were spatially coincident. This raises the question of whether or not the IIM is a reasonable measure of interactions, and in particular, if it could simply be the case that it is dominated by single encounters.

We investigate this in Fig. 3, where we examine the correlation between the IIM and the number $N_{\rm enc}$ of 'tidal encounters' as quantified by calculating the tidal radius of a given satellite *induced by one of the other satellites* (Knebe et al. 2004). Whenever the tidal

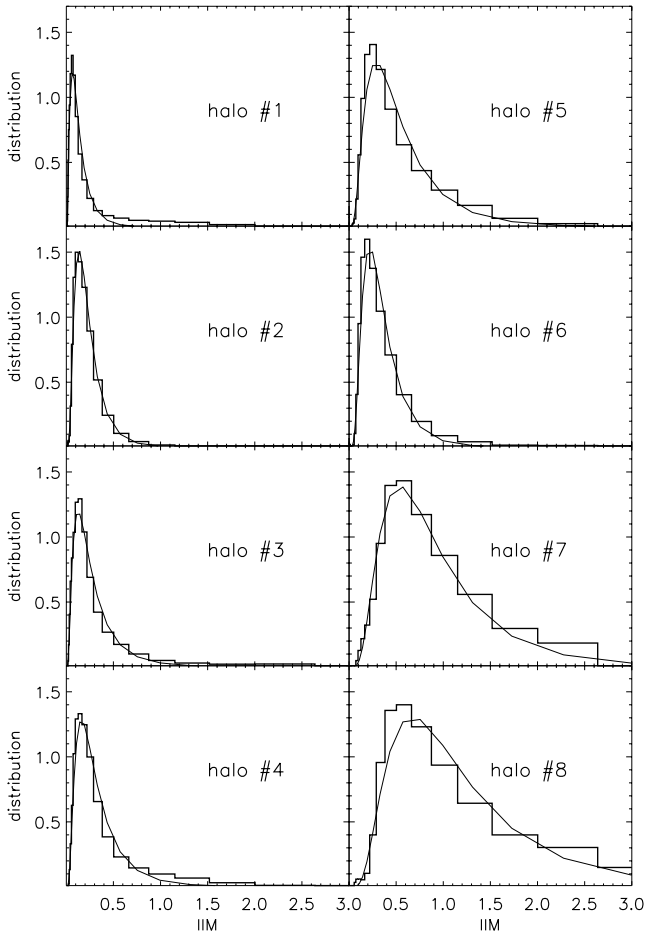

Figure 2. Frequency distribution of the IIM.

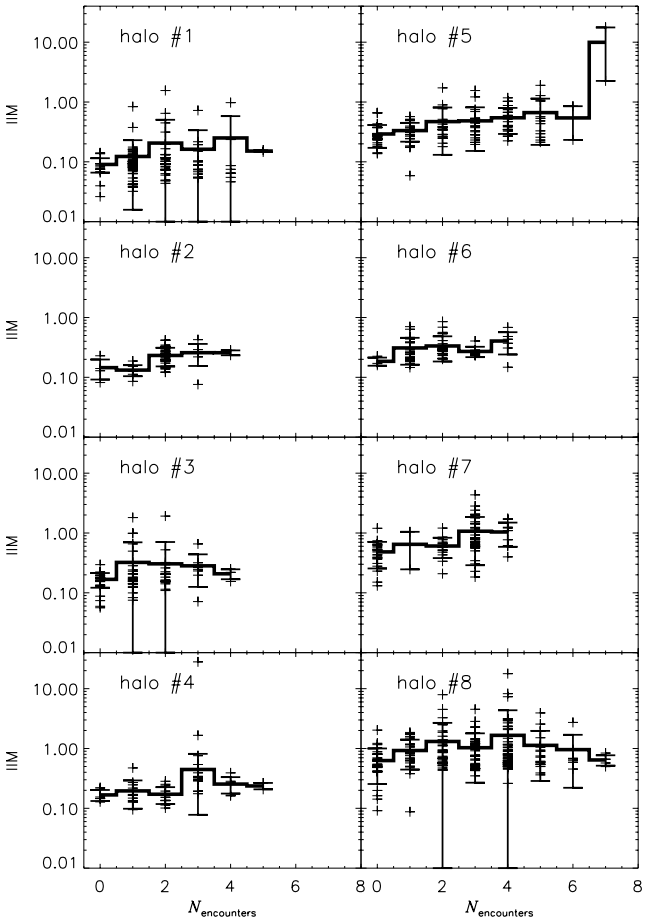

Figure 3. Correlation of IIM with the number of encounters as defined in the text.

Table 1. Best-fitting parameters of IIM distribution to lognormal.

Halo	Age (Gyr)	IIM_{peak}	IIM_0	σ_0
# 1	8.30	0.067	0.118	0.756
# 2	7.55	0.137	0.199	0.614
# 3	7.16	0.126	0.227	0.767
# 4	7.07	0.162	0.270	0.716
# 5	6.01	0.287	0.464	0.692
# 6	6.01	0.221	0.307	0.575
# 7	4.52	0.535	0.789	0.623
# 8	3.42	0.672	1.021	0.646

radius becomes smaller than the radius[2] of the satellite we increment a counter N_{enc} for that particular satellite that keeps track of the number of (perturbing) interactions with companion satellite galaxies.

Fig. 3 clearly indicates that there is little (if any) correlation between the number of satellite–satellite encounters and the IIM *for a single satellite*. Moreover, also the scatter about the mean IIM value in each N_{enc} bin is not affected by the actual number of encounters experienced by the satellite. This strongly suggests that the IIM value is not dominated by single events but rather is a cumulative quantity that is accrued over the lifetime of a satellite. However, we stress that there is a correlation between the width of the distribution of encounters per orbit (cf. fig. 3 in Knebe et al. 2004) and the peak IIM value; although the IIM is not driven by single violent encounters, the greater the number of such events, the higher the IIM of the satellite. However, these arguments are based upon the assumption that the 'strength' of individual encounters is more or less equal. It still appears possible for *one single strong* encounter to dominate the value of IIM.

Another factor possibly affecting the observed correlation between host halo age and interaction measure IIM is the mass fraction of satellites. A simple check indicates that the younger the host the higher the fraction of mass locked up in satellite galaxies. This suggests that the IIM values may in fact be influenced by the most massive subhaloes. We will come back to this point later in Section 3.4 but can already confirm that the distributions presented in Fig. 2 practically remain unaltered if we discard all satellites less massive than 1 per cent of the host's virial mass,[3] denoting the importance of massive subsystems.

In addition, we have investigated whether or not there exists a relation between the IIM and either the eccentricity of a satellite's

[2] We define the radius of a satellite either to be the virial radius, i.e. the radius where the mean averaged density (measured in terms of the cosmological background density ρ_b) drops below $\Delta_{vir}(z)$, or the truncation radius, i.e. the point where the satellite's density profile rises again due to the embedding in the host halo.

[3] One needs to bear in mind that the mass spectrum of subhaloes extends down to as low as 10^{-4}–10^{-5} $M_{vir,host}$ (e.g. DeLucia et al. 2004).

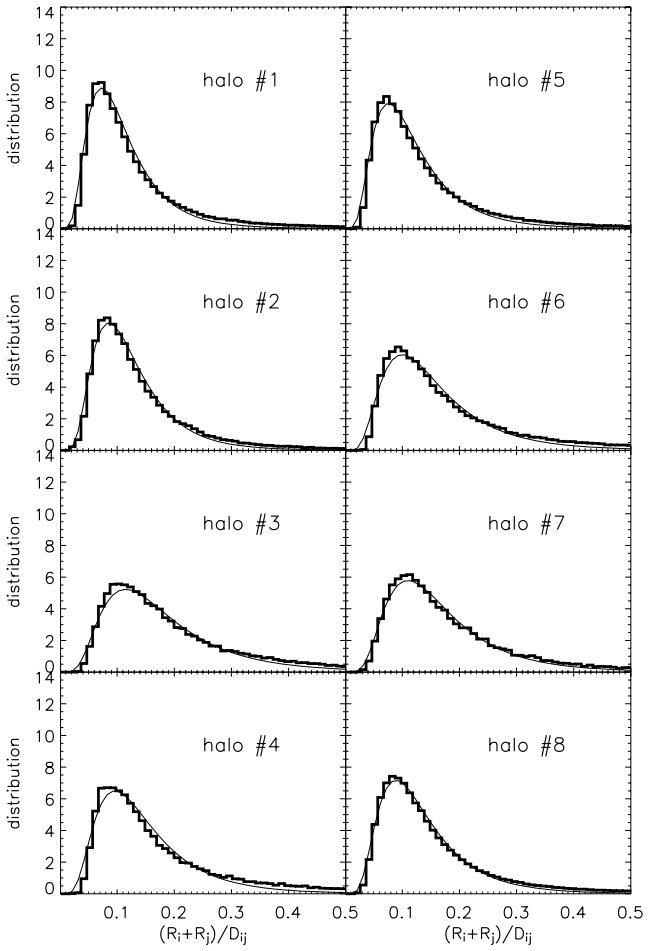

Figure 4. Distribution of the distance of two satellites normalized by the sum of their individual radii; data from each host halo are stacked for all available outputs.

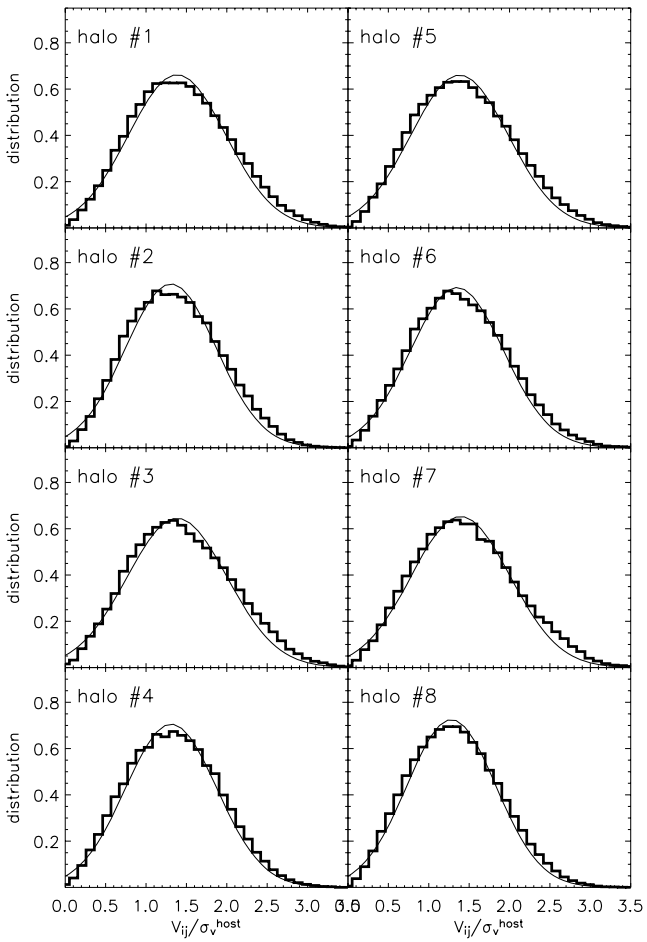

Figure 5. Distribution of the relative velocity of two satellites normalized by the host's velocity dispersion; for each host halo we stack the data from all available outputs.

orbit or its pericentric distance, but we do not find strong evidence for such a correlation. Although we observed a significant drop in the number of encounters per orbit with increasing distance from the host's centre, we find no comparable result for the IIM. This indicates that satellites 'encounter' each other with greater frequency closer to the centre of the host, but that such encounters occur with high relative velocities and so cause little structural damage. *Encounters in the central regions are therefore no more damaging than those in the outer regions*. We elaborate upon this in greater detail in the following section.

3.2 Distributions of relative encounters

We have calculated the distribution of satellite–satellite distances $D_{i,j}$ as well as the relative speed of satellite pairs $V_{i,j,}$ for all available outputs in-between formation redshift $z_{\rm form}$ of the host and $z = 0$, and show the resulting distributions of in Figs 4 and 5, respectively.

In Fig. 4, we have plotted the relative separation $D_{i,j}$ normalized by the sum of the two virial radii of the respective satellites, i.e. R_i and R_j; a value of $(R_i + R_j)/D_{i,j} > 1$ corresponds to a distance of the satellite$_i$–satellite$_j$ pair for which the 'virial spheres' of the satellites i and j are overlapping. We note that the distributions can be fitted by a lognormal distribution:

$$n(x) = \frac{1}{(x/x_0)\sqrt{2\pi\sigma_0^2}} \exp\left(-\frac{\ln^2(x/x_0)}{2\sigma_0^2}\right), \quad (6)$$

where $x = (R_i + R_j)/D_{i,j}$. Fig. 4 is accompanied by Table 2 where we summarize the best-fitting parameters. Despite the age–IIM relation found in the previous Section 3.1 we do not observe any trend for relative distances to increase (or decrease) with halo age. Tormen, Diaferio & Syer (1998) performed a similar analysis, but their respective distance distribution peaks for values corresponding to distances smaller than the sum of the two individual radii indicating they had 'at least one penetrating encounter' (cf. fig. 7 in their paper noting that they are plotting the inverse of our distance measure). However, we note that the definition for a satellite's virial radius used by Tormen et al. (1998) differs to ours; they define the virial radius to be the satellite's radius at the moment it 'merges' with the host halo, whereas we calculate the satellite's radius for each snapshot we have along its orbit within the host halo. This naturally leads to smaller radii as most of the satellites loses mass as it orbits within the denser environment of the host (cf. definition for satellite radius in Section 3.1.1, footnote 2), and as a result the distribution of relative distances peaks at larger separations.

Relative velocities between satellites can also enhance the impact of interactions on mass loss – the slower the encounter between a pair of satellites, the longer the time-scale over which damage can

Table 2. Best-fitting parameters for relative distance distribution.

Halo	x_0	σ_0
# 1	0.097	0.536
# 2	0.111	0.510
# 3	0.158	0.567
# 4	0.130	0.550
# 5	0.104	0.568
# 6	0.137	0.564
# 7	0.147	0.543
# 8	0.119	0.540

Table 3. Best-fitting parameters for relative velocity distribution.

Halo	w_0	σ_0
# 1	1.390	0.563
# 2	1.319	0.544
# 3	1.385	0.572
# 4	1.323	0.548
# 5	1.386	0.564
# 6	1.358	0.548
# 7	1.396	0.562
# 8	1.292	0.534

be done. In Fig. 5, we show the distribution of relative velocities for pairs of satellites, normalized by the velocity dispersion of the host halo. As before, we stack data for all available outputs for each system, but we now fit the distributions with a Gaussian:

$$n(w) = \frac{1}{\sqrt{2\pi\sigma^2}} \exp\left(-\frac{(w-w_0)^2}{(2\sigma^2)}\right). \quad (7)$$

Here $w = V_{\rm rel}/\sigma_v^{\rm host}$ is the relative velocity of two satellites in terms of the velocity dispersion of the host halo. This figure suggests that there is no correlation of peak value with age, in good agreement with the best-fitting parameters presented in Table 3.

In summary, our analysis indicates that slow and/or close penetrating encounters between pairs of satellite galaxies are relatively rare events. We have checked to ensure that our decision to stack all available outputs does not bias our result by masking a potentially interesting signal; however, we can confirm that the results are unaffected whether we construct the distribution from data obtained at a single redshift (e.g. final redshift $z = 0$ or formation redshift $z_{\rm form}$).

3.3 Mass loss induced by satellite–satellite interactions

We have defined a physically motivated quantitative measure of interactions between satellite galaxies in the form of the IIM (equation 3). Our detailed investigation of IIM values in the previous sections provided great insight into the relevance of interactions in general; we were able to demonstrate that satellites encounter other satellites with the same relative velocities and separations at all times during the formation of a cluster, but the interaction measure IIM is higher in younger systems. However, it is difficult to conceive of a means to reconstruct IIM values for satellite galaxies from observational data. Whereas IIM values can readily be evaluated in N-body simulations providing a gauge for the presence and importance of interactions, respectively, we prefer to construct a new measure for quantifying the impact of interactions more applicable to observational data sets. The mass loss suffered by a satellite as a result of the interactions would seem a promising approach; it can be probed observationally, such as in the field of 'galactic archaeology' where tidally stripped (stellar) streams have proven to be a powerful tool (e.g. Helmi et al. 1999). However, understanding the evolution of satellite galaxies is complicated because changes are driven not only by the tidal field of the host (as shown by Knebe et al. 2005) but also by more subtle processes such as the time evolution of the underlying host potential. Explicitly accounting for such time dependency gives better agreement with self-consistent modelling of satellites in the integrals-of-motion space, but there still remains a certain amount of disagreement between the observed and measured mass losses; for example, Knebe et al. (2005) speculated that this can be attributed to either the shape of the host and/or interactions with companion satellites. Using the ideas and prescriptions developed in Section 3.1, we now extend our analysis to place constraints on the mass loss that can be induced by satellite–satellite interactions. A satellite i suffers a mass loss of

$$\Delta M^i = M^i(t_1) - M^i(t_2) \quad (8)$$

between two consecutive outputs t_1 and t_2. We wish to relate a fraction of this mass loss to interactions between satellites and so we write ΔM^i as the sum of the mass loss induced by interactions with other satellites, $\Delta M^i_{\rm sat}$, and with the host halo, $\Delta M^i_{\rm host}$:

$$\Delta M^i = \Delta M^i_{\rm sat} + \Delta M^i_{\rm host}\,. \quad (9)$$

In order to break the degeneracy between $\Delta M^i_{\rm sat}$ and $\Delta M^i_{\rm host}$, we assume that the satellites are point masses M with velocity $\boldsymbol{v}$, and hence write their momentum change $\Delta\boldsymbol{p}$ as follows:

$$\Delta\boldsymbol{p} = \boldsymbol{v}\Delta M + M\Delta\boldsymbol{v} = \boldsymbol{F}\Delta t\,, \quad (10)$$

which can be re-arranged to give

$$\Delta M = (\boldsymbol{F}\cdot\boldsymbol{v}\Delta t - M\Delta\boldsymbol{v}\cdot\boldsymbol{v})/v^2\,, \quad (11)$$

where we (numerically) confirmed that on average $\langle\boldsymbol{F}\cdot\boldsymbol{v}\Delta t\rangle \approx 7\,\langle M\Delta\boldsymbol{v}\cdot\boldsymbol{v}\rangle$ and can therefore simplify the equation for mass loss to read

$$\Delta M^i \propto \left(\frac{\boldsymbol{F}(t_m)\cdot\boldsymbol{v}(t_m)}{v^2(t_m)}\Delta t\right)^{\alpha}, \quad (12)$$

where t_m is the midpoint between two outputs calculated using equation (4) and α is a 'tuning factor' accounting for the approximate nature of our approach. From Fig. 6, we conclude that $\alpha \sim 1/3$ is the most appropriate value (represented by the solid line) and this is the value we adopt in the following analysis.

We now use equation (9) and the scaling relation equation (12) to compute the mass loss suffered as a result of satellite interactions and the influence of the host, respectively:

$$\Delta M^i_{\rm sat} = \frac{\Delta M^i}{1 + \left(\left(\boldsymbol{F}^i_{\rm host}(t_m)\right)\cdot\boldsymbol{v}(t_m)\right)\Big/\left(\boldsymbol{F}^i_{\rm sat}(t_m)\cdot\boldsymbol{v}(t_m)\right)^{\alpha}},$$
$$\Delta M^i_{\rm host} = \frac{\Delta M^i}{1 + \left(\left(\boldsymbol{F}^i_{\rm sat}(t_m)\cdot\boldsymbol{v}(t_m)\right)\Big/\left(\boldsymbol{F}^i_{\rm host}(t_m)\cdot\boldsymbol{v}(t_m)\right)\right)^{\alpha}}, \quad (13)$$

where we have further assumed that equation (12) holds for both the force due to satellite–satellite interactions and the force induced by the host halo.

Over the years, a number of sophisticated prescriptions for modelling tidally driven mass loss have been developed, largely within

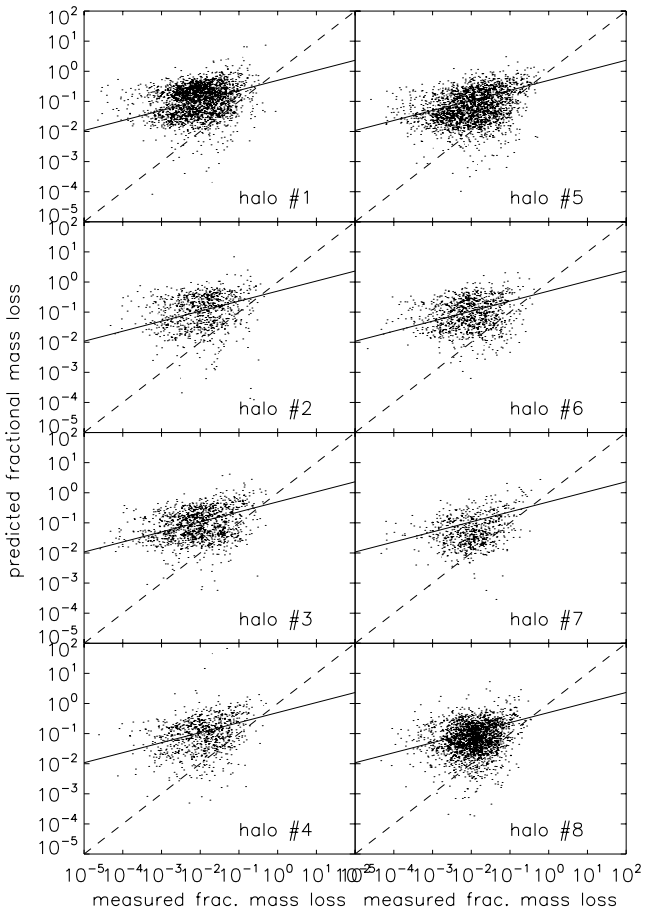

Figure 6. Measured fractional mass loss in between two consecutive outputs versus the predicted mass loss as given by equation (12). The solid line represents a $x^{1/3}$ power law whereas the dashed line indicates a simple 1:1 relation $x^{1.0}$.

the context of the evolution of globular clusters in external tidal fields (e.g. Spitzer 1958; Gnedin, Lee & Ostriker 1999, and references therein) but also for understanding the disruption of satellite galaxies in cosmological dark matter haloes (e.g. Taylor & Babul 2001; Hayashi et al. 2003; Penarrubia & Benson 2005). Although equation (13) represents a first-order approximation for the mass loss, we will demonstrate that our formulae lead to qualitatively correct results and predictions with the right order of magnitude; a more thorough study and the development of a full theoretical model for mass loss in cosmological dark matter haloes will be dealt with in a companion paper. In the present study, we concentrate on quantifying the importance of interactions for mass loss and their importance for analytical modelling in galactic archaeology.

In the following analysis, we use the average fractional mass loss per Gyr for a given satellite i,

$$\left\langle \frac{\mathrm{d}M}{M\mathrm{d}t} \right\rangle^{i} = \frac{1}{N_t^i} \sum_{t=t_i}^{t_{\rm now}} \frac{M_t^i - M_{t-1}^i}{M_t^i} \frac{1}{\Delta t}, \tag{14}$$

where N_t^i is the number of outputs available for that particular satellite between the time it enters the host and the present; the time interval Δt is calculated for two consecutive outputs. We are using equation (13) to split mass loss due to encounters and the influence of the host. The resulting distributions for average mass loss per Gyr are shown in Fig. 7. This figure demonstrates that the mass loss induced by encounters between satellite galaxies can be as important as the tidal stripping of mass by the host potential in dynamically young systems. However, as the system becomes more relaxed, the relevance of such interactions becomes progressively less important and a significant fraction of the mass loss can be directly ascribed to the tides induced by the host. Table 4 accompanies Fig. 7; here we have calculated the mean of the average mass loss per Gyr for all satellites in a given host halo:

Table 4. The mean average fractional mass loss per Gyr when averaging over all times and all satellites in a halo. The last column measures the contribution from satellite–satellite interactions, i.e. $f_{\rm sat} = \overline{\langle \mathrm{d}M/M\mathrm{d}t \rangle_{\rm sat}} / \overline{\langle \mathrm{d}M/M\mathrm{d}t \rangle_{\rm total}}$.

Halo	$\overline{\langle \mathrm{d}M/M\mathrm{d}t \rangle_{\rm total}}$	$\overline{\langle \mathrm{d}M/M\mathrm{d}t \rangle_{\rm sat}}$	$\overline{\langle \mathrm{d}M/M\mathrm{d}t \rangle_{\rm host}}$	$f_{\rm sat}$
# 1	0.132	0.030	0.102	0.23
# 2	0.123	0.033	0.090	0.27
# 3	0.143	0.039	0.104	0.27
# 4	0.126	0.038	0.088	0.30
# 5	0.147	0.050	0.097	0.34
# 6	0.137	0.041	0.096	0.30
# 7	0.141	0.054	0.087	0.38
# 8	0.123	0.055	0.068	0.45

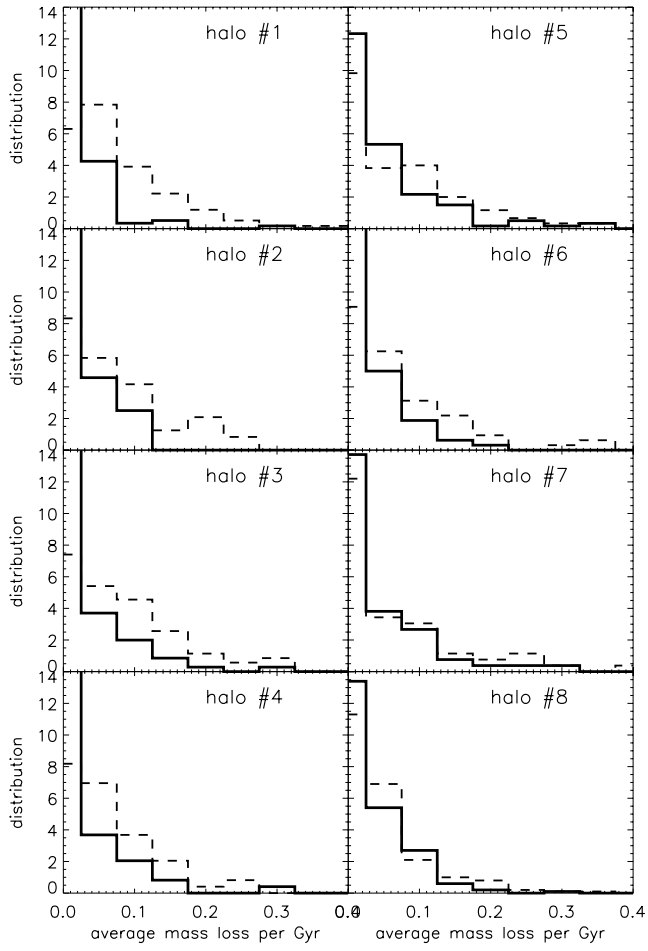

Figure 7. Frequency distribution of the average (fractional) mass loss per Gyr. The thick solid line shows mass loss due to satellite interactions and the dashed line due to the influence of the host alone.

$$\overline{\left\langle \frac{\mathrm{d}M}{M\,\mathrm{d}t} \right\rangle} = \frac{1}{N_{\rm sat}} \sum_{i=1}^{N_{\rm sat}} \left\langle \frac{\mathrm{d}M}{M\,\mathrm{d}t} \right\rangle^{i}. \tag{15}$$

From Table 4, we infer that the mass loss induced by satellite–satellite encounters can amount to as much as 45 per cent of the total mass loss experienced by a single satellite. Even though the IIM (as defined by equation 3) and its distribution in Fig. 2 indicated a rather low importance of such interactions the conversion to mass loss reveals a more pronounced influence due to the observed power-law scaling $\Delta M \propto (F\,\Delta t)^{\alpha}$ with $\alpha \sim 1/3$. However, the results are robust to changes in the power-law index, e.g. changing the exponent from 1/3 to unity gives us the range from 15 per cent mass loss due to interactions for the oldest host (halo # 1) up to 40 per cent for the youngest system (halo # 8).

3.4 A test scenario: host halo # 8

Two questions remain unanswered.

(i) Why do we observe a higher mass loss due to interactions in younger systems?
(ii) Can our results be verified?

The most natural approach to addressing these questions involves explicitly tracking the mass loss of an individual satellite as a function of time and factoring out the influence of the other satellites. To do this, we have performed two additional simulation runs of halo #8, both starting at its formation redshift $z = 0.3$. In the first, we have removed all haloes bar the progenitor of the $z = 0$ host halo and one particular satellite that happened to have a rather high interaction value of IIM = 8.3; our analysis indicates that about 40 per cent of its average mass loss per Gyr was induced by interactions with other satellites. In the second run, we removed only those subhaloes that have not merged with the host's progenitor at redshift $z = 0$ except our test satellite'. We refer to these runs as 'fully cleaned' (the former, including *only* the host and our test satellite) and 'cleaned' (the latter, also including the massive subhaloes merging with the host), respectively.

A visual impression of the initial setup of the cleaned run is given in (the upper left-hand panel of) Fig. 10 which nicely demonstrate the 'smoothness' of the cleaned simulation. The satellite in question is marked by a blue circle.

For each of the three runs, we closely follow the mass loss history of this satellite and the resulting curve (normalized to the initial mass) is presented in Fig. 8. Note that we identify the set of particles that are bound to the satellite at the initial time and we explicitly track these particles through subsequent snapshots, checking what fraction are bound to the satellite at later times. This avoids any difficulties that may arise from attempting to identify the bound mass of the satellite as it is identified in subhalo catalogues constructed for consecutive snapshots. For each available output, we find the new satellite centre by using the centre-of-mass of the innermost bound particles as a first guess for the central density peak. We then iteratively remove all of the satellite's particles that are not gravitationally bound. Fig. 8 shows that the mass loss suffered by the satellite is significantly reduced in both of the cleaned runs. However, we stress that removing all substructure not only affected the satellite under investigation but also the overall dynamics of the host, especially for the fully cleaned run: host halo # 8 can be classified as a violent (triple) merger in the original cosmological simulation and removing all of its progenitors must clearly leave an imprint on its (internal) dynamics. Nevertheless, we note that although the

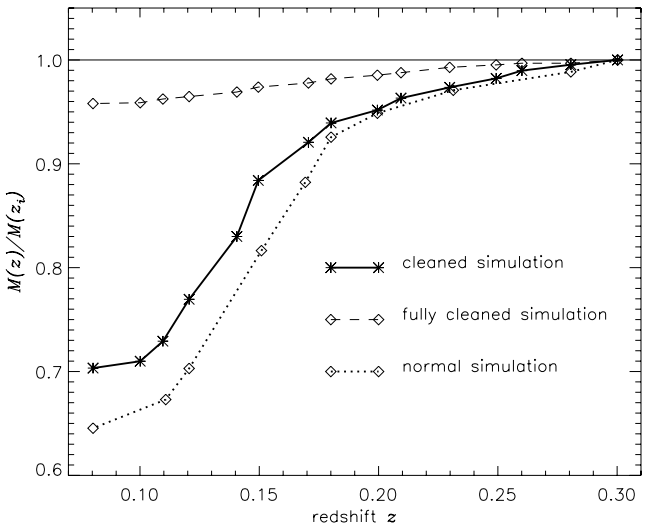

Figure 8. Tracking the mass of the subhaloes indicated by the red circle in Fig. 10 from initial redshift $z = 0.31$ to 0.08 through the actual ('normal') simulation as well as out two test cases described in Section 3.4.

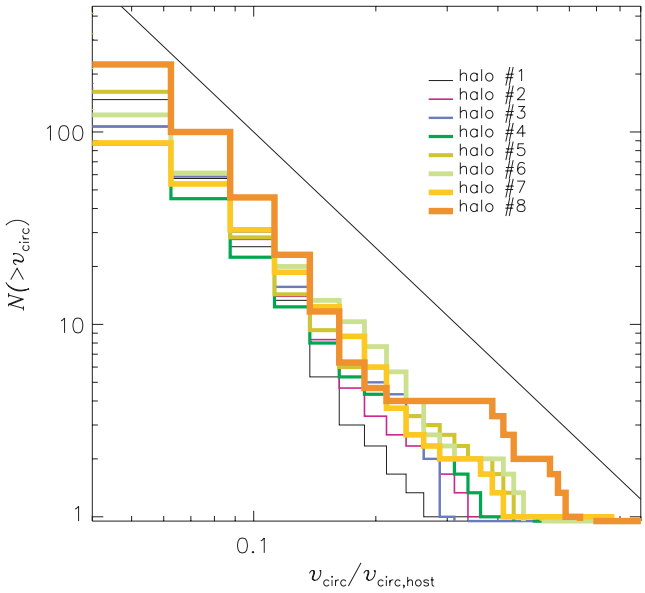

Figure 9. Cumulative circular velocity distribution for all subhaloes in the eight host haloes half way through the evolution from redshift $z = z_{\rm form}$ to 0. The solid line represent the power law x^{-2}.

'cleaned' run retained most of its high-mass substructures, we observed a trend for the mass loss to decrease.

This simple test has demonstrated that the principal driver for interaction induced mass loss is the mass spectrum of the substructure haloes. We may strengthen this statement further by considering the cumulative circular velocity distribution presented in Fig. 9. Noting that the maximum circular velocity is a reasonable measure of halo mass, we conclude from this figure that a sizeable fraction of the mass in satellites in each of the eight host haloes is bound to high-mass systems roughly half way through their evolution (i.e. $t = (t_{\rm form} + t_0)/2$).

These massive subhaloes are likely to be responsible for the increased mass loss due to interactions, as already indicated by Fig. 8. We can investigate this assertion by determining the fraction of

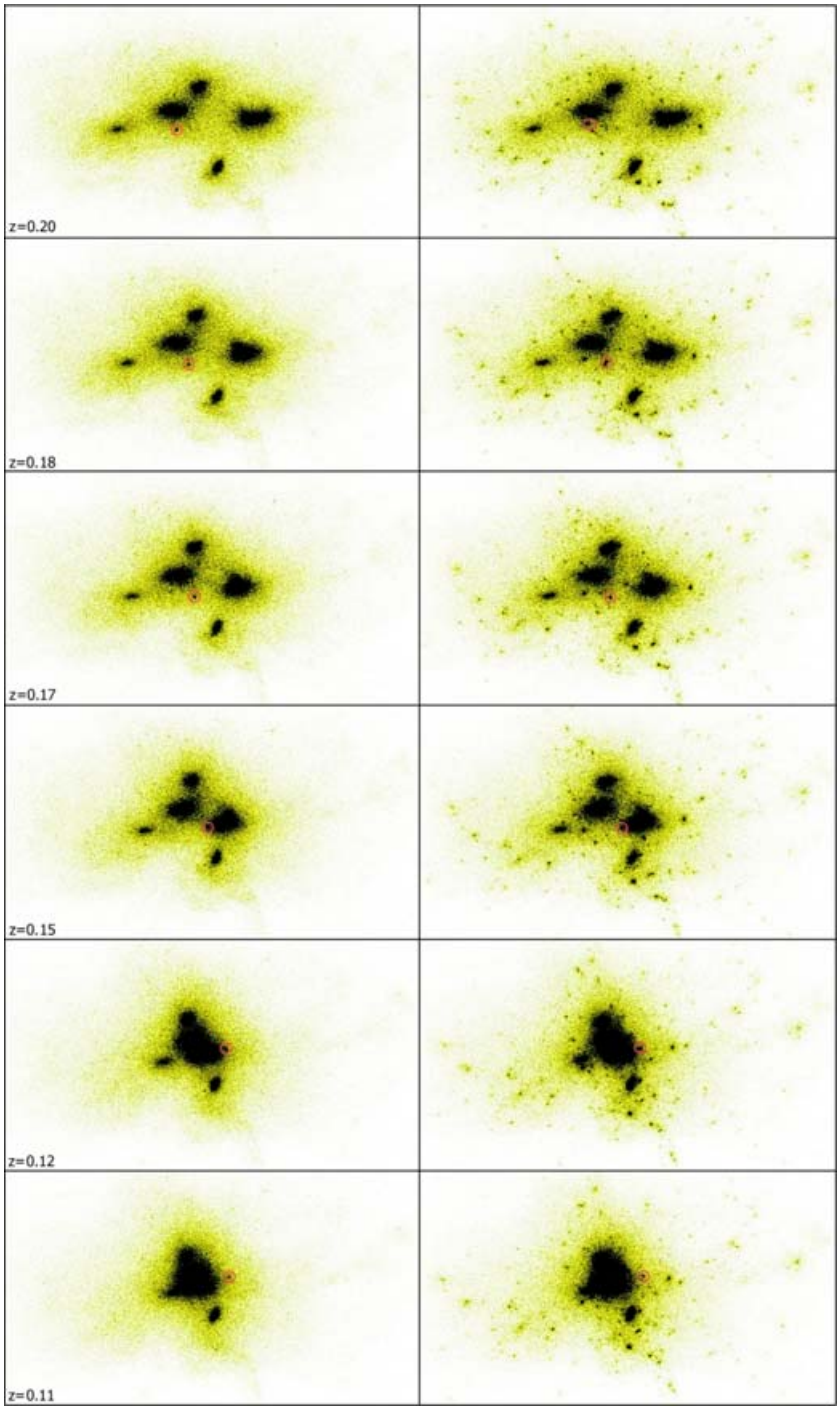

Figure 10. Several snapshots of the actual simulation of halo # 8 (right-hand panel) and the resimulation cleaned of all (but one) subhalo not ending up in the host at $z = 0$. The subhalo visible to the lower right of the host happens to be a foreground objects not interfering with the system under investigation.

the IIM measure that is due to massive satellites. As already mentioned in Section 3.1, we can reproduce the distributions of IIM values presented in Fig. 2 by including only those satellite galaxies that are more massive than 1 per cent of the host's virial mass.[4] This indicates quite clearly that the IIM values are dominated by more massive systems and the contribution of low-mass satellites is negligible.

4 CONCLUSIONS

The hierarchical manner in which structure in our Universe forms – from the bottom up, through mergers and accretions – implies that interactions between galaxies (and consequently, between their

[4] Using an empirically derived scaling relation between satellite mass and maximum circular velocity, i.e. $v_{\rm circ} \propto M^{1/3}$, the mass limit of 1 per cent $M_{\rm vir,host}$ corresponds to a cut in circular velocity at around 20 per cent $v_{\rm circ,host}$ (cf. Fig. 9).

dark matter haloes) are commonplace. These interactions have been invoked to explain, for example, galaxy transformation (e.g. Moore et al. 1998), the exchange of angular momentum (e.g. Barnes & Efstathiou 1987), the triggering of star bursts (e.g. Mihos & Hernquist 1994) and morphological change (Steinmetz & Navarro 2002). The impact of interactions between satellite galaxies and their massive host on the structure of the satellites has been studied in some detail (e.g. Hayashi et al. 2003), but less well understood is the role played by interactions between satellite galaxies; in other words, the impact of satellite–satellite interactions. This important topic has formed the basis of this paper.

We have defined an *integral interaction measure* (IIM) that allows us to quantitatively measure the importance of interactions between satellite galaxies for their mass loss. Our definition allows us to gauge the relative contributions of the host potential and other satellites for the mass loss suffered by an individual satellite. We have shown that the distribution of IIMs for a population of satellites within a cluster mass dark matter halo can be characterized as log-normal, and that the peak value (or mode) correlates with the age of the host system – typically the younger the host, the larger the peak IIM. Moreover, we note that the relative width of the distribution is broader in younger systems. We were able to confirm that the most significant contribution to the interaction measure comes from massive companion satellites which naturally explain the correlation with host age: subhaloes in young clusters have larger masses relative to the host since they have not been tidally disrupted yet which is validated by the observation that our younger hosts have a higher mass fraction in satellites. However, the IIM values are generally much less than unity, implying that the bulk of the mass loss suffered by a satellite is driven by its interaction with the host potential. We have also shown that, in those cases where the IIM is large, it cannot be due to single encounters; rather, it is built up through a series of many encounters.

Our investigations have also extended the result of Knebe et al. (2004) by demonstrating that not only are penetrating encounters between satellite galaxies relatively rare events over the 'lifetime' of a cluster,[5] but that the time-scale of such encounters is short, i.e. the relative velocities are typically of order the one-dimensional velocity dispersion of the host. This result may be of interest to those engaged in developing semi-analytic models of galaxy formation because we might expect the severity of encounters between satellites to be important for the efficiency of starbursts arising from tidal interactions.

Finally, we have proposed a simple *empirical* model for separating the respective contributions of the host potential and interactions with other satellites for the mass loss suffered by a satellite. Our model suggests that mass loss driven by satellite interactions can be significant – in the particular test case we considered, we have shown that a given satellite can lose as much as $\sim$40 per cent of its initial mass. This may appear surprising at first, but we have shown that the IIM is a cumulative measure and so while damaging encounters are relatively rare occurrences, a large number of 'weak' interactions can affect the structure of a satellite and drive the mass loss it suffers. However, we stress that this empirical model should be taken as simple guide providing an 'order-of-magnitude' estimate of the mass loss, and a more sophisticated model is required; this will be the focus of future work.

[5] I.e. since its formation redshift.

ACKNOWLEDGMENTS

The simulations presented in this paper were carried out on the Beowulf cluster at the Centre for Astrophysics & Supercomputing, Swinburne University. AK acknowledges funding through the Emmy Noether Programme by the DFG (KN 722/1). CP thanks Virginia Kilborn and Sarah Brough for helpful discussion. The financial support of the Australian Research Council is gratefully acknowledged.

REFERENCES

Barnes J. E., 1988, ApJ, 331, 699
Barnes J. E., Efstathiou G., 1987, ApJ, 319, 575
Bekki K., Chiba M., 2005, MNRAS, 356, 680
Connors T. W., Kawata D., Gibson B. K., 2005, MNRAS, submitted (astro-ph/0508390)
De Lucia G., Kauffmann G., Springel V., White S. D. M., Lanzoni B., Stoehr F., Tormen G., Yoshida N., 2004, MNRAS, 348, 333
Gao L., De Lucia G., White S. D. M., Jenkins A., 2004, MNRAS, 352, L1
Gardiner L. T., Noguchi M., 1996, MNRAS, 278, 191
Gill S. P. D., Knebe A., Gibson B. K., 2004a, MNRAS, 351, 399
Gill S. P. D., Knebe A., Gibson B. K., Dopita M. A., 2004b, MNRAS, 351, 410
Gill S. P. D., Knebe A., Gibson B. K., 2005, MNRAS, 356, 1327
Gnedin O. Y., Lee H. M., Ostriker J. P., 1999, ApJ, 522, 935
Goto T., 2005, MNRAS, 357, 937
Hayashi E., Navarro J. F., Taylor J. E., Stadel J., Quinn T., 2003, MNRAS, 584, 541
Helmi A., 2004, MNRAS, 351, 643
Helmi A., White S. D. M., de Zeeuw P. T., Zhao H., 1999, Nat, 402, 53
Ibata R. A., Lewis G. F., 1998, ApJ, 500, 575
Ibata R., Irwin M. J., Lewis G. F., Ferguson A. M. N., Tanvir N., 2003, MNRAS, 340, L21
Ibata R., Chapman S., Ferguson A. M. N., Lewis G., McConnachie A., 2004, MNRAS, 351, 117
Knebe A., Green A., Binney J., 2001, MNRAS, 325, 845
Knebe A., Gill S. P. D., Gibson B. K., 2004, Publ. Astron. Soc. Aust., 21, 216
Knebe A., Kawata D., Gill S. P. D., Gibson B. K., 2005, MNRAS, 357, L35
Lin D. N. C., Jones B. F., Klemola A. R., 1995, ApJ, 439, 652
Mastropietro C., Moore B., Mayer L., Wadsley J., Stadel J., 2005, MNRAS, 363, 521
Mihos J. C., Hernquist L., 1994, ApJ, 425, L13
Mihos J. C., Harding P., Feldmeier J., Morrison H., 2005, ApJ, 631, L41
Moore B., Lake G., Katz N., 1998, ApJ, 495, 139
Navarro J. F., Helmi A., Freeman K. C., 2004, ApJ, 601, L43
Odenkirchen M. et al., 2003, AJ, 126, 2385
Oh K. S., Lin D. N. C., Aarseth S. J., 1995, ApJ, 442, 142
Penarrubia J., Benson A. J., 2005, MNRAS, 364, 977
Spitzer L., 1958, ApJ, 127, 17
Steinmetz M., Navarro J. F., 2002, New Astron., 7, 155
Taylor J. E., Babul A., 2001, ApJ, 559, 716
Toomre A., Toomre J., 1972, ApJ, 178, 623
Tormen G., Diaferio A., Syer D., 1998, MNRAS, 299, 728
Yoshizawa A. M., Noguchi M., 2003, MNRAS, 339, 1135
Yun M. S., Ho P. T. P., Lo K. Y., 1994, Nat, 372, 530
Zhao H., 1998, ApJ, 500, L149

This paper has been typeset from a TEX/LATEX file prepared by the author.